


Model-based Scale Up of Solid Bowl Centrifuges Using Experimentally Determined Material Functions

Ouwen Zhai^{1,‡,*}, Helene Baust^{1,‡}, Marco Gleiß¹, and Hermann Nirschl¹

DOI: 10.1002/cite.202200117

 This is an open access article under the terms of the Creative Commons Attribution-NonCommercial-NoDerivs License, which permits use and distribution in any medium, provided the original work is properly cited, the use is non-commercial and no modifications or adaptations are made.

Dedicated to Prof. Dr.-Ing. Joachim Werther on the occasion of his 80th birthday

The scale up of solid bowl centrifuges is a major challenge as the process and material behavior are complex and difficult to describe. A common approach to forecast the process behavior is to use analytical models and transfer the experience gained from the lab to the industrial scale. In this context, time-consuming and cost-intensive pilot scale experiments are necessary. This paper presents a methodology to improve the scale up process and make it more sustainable by using a numerical model that allows the real-time tracking of the process and a more reliable scale up process. For this approach, the material behavior is derived from laboratory experiments whereby the scalability is given. Here, the determination of material functions allows an accurate representation of the material behavior for solid bowl centrifuges of different scales. The focus of this paper is the detailed explanation of material related functions for the scale up of decanter centrifuges.

Keywords: Decanter centrifuge, Material characterization, Modelling, Separation technology

Received: June 27, 2022, *revised:* October 05, 2022; *accepted:* November 16, 2022

1 Introduction

A basic unit operation in process engineering is the mechanical fluid separation. Solid bowl centrifuges are often used for thickening, classifying and dewatering of finely dispersed particles. As part of an industrial process chain, their usage requires a sufficiently accurate prediction of the product and machine behavior. One challenge in the design of solid bowl centrifuges is the scale up from the lab to the industrial scale as different parameter combinations of the process behavior lead to the same separation result, while changes in the operating conditions have different effects on the performance of the machine [1]. As a result, it is not possible to simply scale up the geometry and process conditions linearly. For a successful scale up, pilot scale tests are necessary which are cost-intensive due to the energy and manpower required.

For the design of solid bowl centrifuges, literature provides mathematical approaches such as the sigma theory [2, 3], the g-volume [4] or the Leung number [5]. Here, the sigma theory is the most commonly used. Ambler [2] describes the separation by equating the mean residence time and the sedimentation time of a single particle in the Stokes regime and transfers the results from lab to industrial scale conditions. Influences such as the solids volume fraction, particle shape, flow conditions, turbulence, or sediment build-up are not considered. Wakeman [4] presents the

g-volume as another approach for the scale up of solid bowl centrifuges allowing the comparison of geometrically similar machines. Leung [5] assumes that a very thin fast-flowing boundary layer exists at the interface between the gas and liquid phase. Due to reasons of mass conservation, a stagnant layer with a neglectable flow in axial direction is formed below the boundary of the rotating pool. Within the boundary layer, Leung calculates the separation based on the Stokes' settling velocity similar to the sigma theory and introduces the Leung number as a dimensionless parameter which allows the scale up of different solid bowl centrifuges [6].

Baust et al. [7], Gleiß et al. [8, 9] and Menesklou et al. [10] exploit the ever-increasing computational power for the design optimization of solid bowl centrifuges. To improve the understanding of the separation process in decanter centrifuges, Baust et al. [7] have developed a method to study the flow in the apparatus. For this purpose, the

¹Ouwen Zhai, Helene Baust, Dr.-Ing. Marco Gleiß, Prof. Dr.-Ing. Hermann Nirschl (ouwen.zhai@kit.edu) Karlsruhe Institut für Technologie (KIT), Institut für Mechanische Verfahrenstechnik und Mechanik (MVM), Straße am Forum 8, 76131 Karlsruhe, Germany.

[‡]Both authors contributed equally to this paper

simulation model takes sedimentation and sediment formation into account. Depending on the solids volume fraction, a distinction is made between the slurry and the sediment, and a different rheological model is assigned to each phase. In contrast, Gleiß et al. [8] have developed a real-time capable dynamic model for tubular and decanter centrifuges and extended common mathematical models by the influence of the forming sediment on the residence time. The flow is adapted by an approximated plug flow with the same residence time behavior as that of the machine to be simulated. Deviations from the ideal plug flow are considered by a component balance for the solid phase, where the interconnection of a predefined number of compartments approximates the non-ideal flow behavior and allows to extend the simulation approach with the real residence time behavior. Consequently, the simulation shows a good agreement with the experiments. Menesklou et al. [10] shows the scalability and transferability of the multi-compartment approach from lab to industrial scale for geometric non-similar decanter centrifuges.

The design of solid bowl centrifuges and the choice of suitable operating conditions depend significantly on the properties of the slurry. One main advantage of the methods presented in this work is that the material characterization is done on a lab scale with a small amount of material. Material functions which describe the material behavior are determined by lab experiments and then implemented in the multi-compartment approach. Here, the real settling behavior is determined instead of assuming Stokes' settling which leads to more accurate predictions of the process compared to the conventional methods. Another advantage of this approach is the capability to gain knowledge about the kinetics of the process due to the spatially- and time-resolved simulation. Therefore, product properties like the particle size distribution and the solids content are obtained for each time step and compartment. As a result, a model is received that supports the process design and allows to describe the process even if the input variables change (see Fig. 1). The medium-term goal is to support the process design and reduce the number of pilot scale tests and thus save costs.

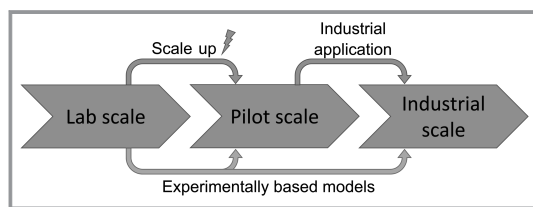


Figure 1. Main idea of process design: Models based on simple lab experiments allow the derivation of material functions. By implementing the material functions in real time models, a targeted support of the scale up is possible. Here, the top path illustrates the path of a conventional scale up and the bottom path the path of a scale up based on experimentally based models.

2 Theoretical Background

2.1 Sedimentation

The sedimentation behavior of particles is essential in the operation of solid bowl centrifuges. How fast the particles settle depends on the liquid and disperse properties. Additionally, the solids content has a significant impact on the settling velocity. There are different approaches to determine the settling velocity. When an infinite dilution is given, the settling velocity of a single spherical particle in a Newtonian fluid is obtained by a force balance considering the drag, buoyancy and weight force. With the assumption of a stationary medium, the settling velocity of a particle u_p in the gravitational field is calculated with the following equation:

$$u_p = \sqrt{\frac{4}{3} \frac{x_p g}{c_D (Re_p)} \frac{\rho_s - \rho_l}{\rho_l}} \quad (1)$$

Here, g is the gravitational acceleration, x_p is the particle diameter, ρ_s and ρ_l are the corresponding densities of the solid and liquid, and c_D is the drag coefficient which depends on the particle Reynolds number Re_p . The particle Reynolds number is the dimensionless correlation of viscosity and inertia forces and depends on the settling velocity of the particle and the dynamic viscosity of the liquid η_l :

$$Re_p = \frac{x_p \rho_s u_p}{\eta_l} \quad (2)$$

For a laminar flow ($Re_p < 0.25$) [11] known as the Stokes' region, the drag coefficient is inversely proportional to the particle Reynolds number:

$$c_D = \frac{24}{Re_p} \quad (3)$$

With the mentioned assumptions and Eq. (1) – (3) the settling velocity according to Stokes $u_{p,Stokes}$ [12] is simplified to the following equation:

$$u_{p,Stokes} = \frac{(\rho_s - \rho_l) x_p^2 g}{18 \eta_l} \quad (4)$$

In centrifuges the acceleration force is significantly higher than the gravitational acceleration. Thus, the centrifugal number C , also called g-force, is used which is the ratio of the centrifugal and gravitational field:

$$C = \frac{R \omega^2}{g} \quad (5)$$

Here, R is the radial position in the centrifuge and ω is the angular velocity. Hence, the settling velocity in a centrifugal field according to Stokes is determined by the following equation:

$$u_{p,\text{Stokes}} = \frac{(\rho_s - \rho_l)x_p^2 R\omega^2}{18\eta_l} \quad (6)$$

As this approach is only valid for very diluted slurries, the hydrodynamic interaction between the particles and fluid for increasing solids content requires another representation of the settling behavior. With increasing solids content, the particles start to form clusters which settle faster due to their larger size. Additionally, smaller particles settle in the slipstream of larger and thus faster settling particles which leads to smaller particles settling faster, too. With even further increasing solids content, the momentum exchange between the particle and fluid starts to have a significant effect which leads to a reduced settling velocity and slower particle settling compared to Stokes' Law [12]. Within the hindered settling regime individual particle settling is prevented and a settling front with a sharp interphase between the clarified liquid and the slurry is formed. A hindered settling function H allows the prediction of the real settling velocity in correlation to the settling velocity according to Stokes. A commonly used approach regarding designing centrifuges is the approach by Richardson and Zaki [13]. As this approach is solely accurate for monodisperse particles, a different approach is needed to describe the influence of polydispersity. According to the approach by Michaels and Bolger [14], a non-linear hindered settling function H containing empirical parameters is able to accurately describe the hindered settling of polydisperse particles. The following equation shows a modified approach by Michaels and Bolger [14] which correlates the real settling velocity with the solids volume fraction ϕ and three empirical parameters r_1 , r_2 , and r_3 .

$$H(\phi) = \frac{u_p}{u_{p,\text{Stokes}}} = r_1 \left(1 - \frac{\phi}{r_2}\right)^{r_3} \quad (7)$$

2.2 Consolidation

During the centrifugation process in solid bowl centrifuges, the driving force for particle settling is the centrifugal force. The settling of the particles leads to particle accumulation and the formation of a liquid saturated sediment. The sediment has a significantly different behavior compared to a slurry. As particle-particle contacts are present within the sediment, particle migration towards the inner wall of the rotor occurs. The transition between particle settling and sediment build-up is abrupt and can be described by the gel point ϕ_{gel} which is a characteristic solids volume fraction where first particle-particle contacts occur. The properties of the formed sediment including its compressibility are heavily dependent on the properties of the particles (e.g., form and size). For the characterization of a sediment's compressibility, the influence of the compression resistance p_s on the sediments structure must be known. In general, sediments

can be divided into incompressible and compressible sediments. On one hand, sediments formed by particles with a particle size $x_p \geq 10 \mu\text{m}$ are generally incompressible which means the compression resistance has no influence on the solids content of the sediment ($\phi \neq f(p_s)$). On the other hand, particles with a particle size $x_p \leq 10 \mu\text{m}$ mostly form compressible sediments whereby the compression is caused by rearrangement, breakage or deformation of the particles in the bulk. Here, the influence of the particle-particle interactions gets increasingly dominant compared to the mass forces. The solids content of compressible sediments is a function of the compression resistance ($\phi = f(p_s)$).

There are different approaches to describe the compression of a material by normal stress using non-linear functions to fit on experimental data. The approach used depends solely on the accuracy of the fit function for the experimental data. Green et al. [15] use a power law to describe the consolidation behavior by correlating the compression resistance with the solids volume fraction, gel point and two material specific empirical parameters ρ_1 and ρ_2 :

$$p_s(\phi) = \rho_1 \left[\left(\frac{\phi}{\phi_{\text{gel}}} \right)^{\rho_2} - 1 \right] \quad (8)$$

This approach is strictly limited to compression by normal stress. Gleich [9] provides a detailed overview of further approaches to describe the compression behavior by normal stress. Apart from compression caused by centrifugal pressure, there is also compression by shear forces within a decanter centrifuge caused by the differential movement of the screw. A ring shear tester allows the determination of this type of compression along with the yield point of the material.

2.3 Flow Behavior of the Sediment

The flow behavior of liquid-saturated sediments significantly influences the process outcome in solid-liquid separation or other transport processes of this type of bulk material. In this context, the characterization of the sediment represents an interdisciplinary field of research between bulk solids mechanics and rheology. At the transition between slurry and sediment, the flow behavior changes abruptly. The reason for this is the particle-particle contact in the formed sediment.

In centrifuges, the sediment faces external forces. Therefore, the sediment may show two forms of motion as a result of force effects [16,17]: flowing and sliding. In the case of flow, the sediment deforms as one continuum. The top is moved horizontally relative to the bottom (bottom is fixed). The relative movement creates velocity gradients throughout the continuum and results in a distortion within the entire sediment. In contrast, during sliding the sediment splits into at least two continua that move away from each

other at uniform velocities. A superposition of both forms of motion is possible.

The flowability of a sediment results from the superposition of Coulomb friction at the particle contacts and the viscous friction effects in the liquid [17, 18, 19]. Thereby, saturated sediments always show a yield point which means they are cohesive. The flow behavior depends on its state of consolidation and the properties of the disperse phase such as particle size distribution, particle shape or the chemical composition [20]. Furthermore, the previous history of the bulk material plays an important role which is the reason for assuming a defined state of consolidation while characterizing bulk materials. For measuring flow locations, ring shear testers are used. Fig. 2 shows the standard measurement procedure. The defined state of consolidation is established by shearing the sediment before measuring the flowability with a normal stress that is higher than the normal stress applied during the actual experiment (preshear). Then, the yield point is determined by shearing (shear to failure).

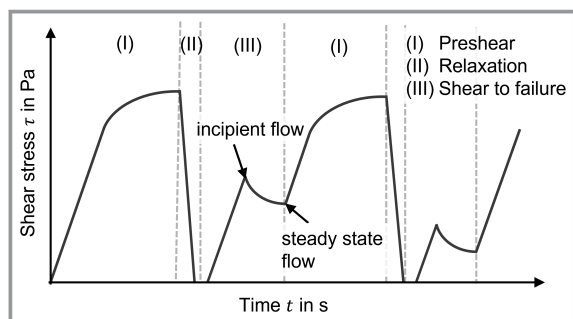


Figure 2. Measurement of yield loci with a ring shear tester: Here, the shear stress τ is measured over the time t during preshear and subsequent shear to failure of a cohesive bulk solid according to Schulze [20].

To characterize liquid-saturated heaps, Hammerich et al. [16] modified a ring shear cell by using filters at the top and the bottom of the shear cell to retain the particles in the cell and a drainage system to ensure complete saturation of the sediment during the shear test. The measurement methodology was adapted from dry bulk mechanics. The pre-consolidated sample passes through both states of incipient and steady state flow. In the case of incipient flow, the sediment starts to move. This state is characterized by a local maximum in shear stress. With further shear, the shear stress decreases until the steady state is reached. In addition, the ring shear tester allows to study the influence of shear on the compression of the sediment. A com-

bination of shear and normal force leads to a higher consolidation of the sediment [21, 22].

2.4 Modeling of Decanter Centrifuges

The methods for designing decanter centrifuges known in the literature are stationary black box models. Gleiß et al. [8] and Menesklou et al. [10] have developed a multi-compartment model for decanter centrifuges which allows the simulation of dynamic process behavior in real-time. Fig. 3 schematically shows the setup of the dynamic model. The simulation domain is the unrolled screw channel of the decanter centrifuge which is then divided into individual compartments with a discrete length Δl . Separation-related material functions are linked with the residence time behavior of the centrifuge whereby two different types of compartments are present: the sedimentation zone and the sediment zone.

The sedimentation zone covers the physical behavior of particle settling. Here, mass balances are solved for a defined number of particle size classes. To solve the component balance of the solid phase, it is assumed that the solid is ideally back-mixed in each balance zone. The component balance is linked to the grade efficiency and the hindered settling function H , the geometric properties of the apparatus and the process conditions.

$$T_i(x, t) = \underbrace{\frac{R_{s,i}(t)}{R_{s,i}(t) - R_w}}_{\text{Geometric parameters}} \left(1 - \exp \left\{ - \frac{(R_{s,i}(t) - R_w) B_c \Delta l}{1} \right\} \right) \underbrace{\frac{\Delta \rho H(\phi, t) x^2}{18 \eta_1}}_{\text{Material characteristics}} \underbrace{\frac{\omega^2}{\dot{V}_{i-1}}}_{\text{Process conditions}} \quad (9)$$

Here, T_i is the grade efficiency, $R_{s,i}$ is the radius of the sediment surface, R_w is the weir radius, B_c is the screw width, Δl the length of one compartment and \dot{V} the volumetric flow rate.

The sediment zone describes the sediment accumulation and the sediment transport whereat the transportability is a

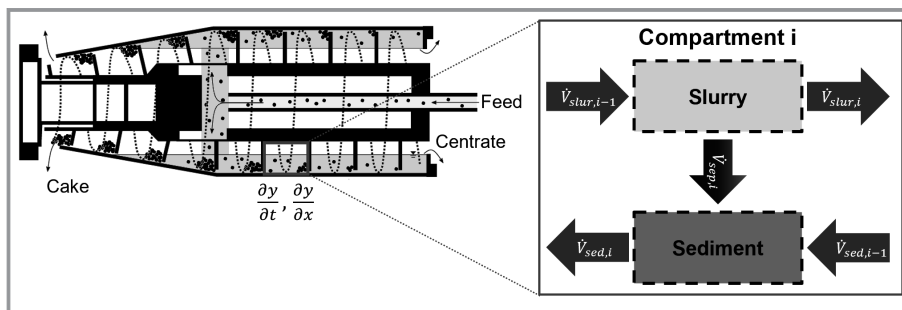


Figure 3. Schematic representation of a multi-compartment model based on a sedimentation zone and a sediment zone to describe the dynamic behavior of solid bowl centrifuges. Adapted with permission of Gleiß [9].

crucial parameter that significantly influences the sediment build-up as well as the transport out of the machine. Most models are limited to the definition of a transport velocity in axial direction [9]. The unsteady behavior depends on the material behavior as well as on the geometry of the screw and the process conditions. The material-dependent variables also include a coefficient of friction. It is usually not measurable which is why a transport efficiency k has been defined in this model to mathematically describe the quality of the sediment transport. It represents the ratio of the actual transport of the sediment to the theoretically possible transport of the sediment corresponding to the differential speed of the screw conveyor. The solids transport velocity \bar{v}_{tr} is calculated on the basis of the differential speed Δn between screw and bowl, the screw pitch angle α and the material behavior which is described by the transport efficiency k :

$$\bar{v}_{tr} = \frac{k B_c \Delta n}{\sin(\alpha)} \quad (10)$$

A more detailed description of the model is given by Gleiß [9].

3 Material Characterization

The methods for the material characterization are shown on two exemplary materials: titanium dioxide (TiO₂) and polyvinyl chloride (PVC). Fig. 4 shows the particle size distributions of the two materials. Here, the median particle size of PVC is $x_{50,3} = 1.96 \mu\text{m}$ while that of TiO₂ is $x_{50,3} = 0.33 \mu\text{m}$.

3.1 Hindered Settling Function

In order to determine the sedimentation behavior, experiments with an analytical centrifuge (LUMiSizer[®] from LUM GmbH) are conducted. Its main components are a rotating disc, a light source and a detector. The measurement principle is based on a space- and time-resolved instantaneous measurement of the absorbance of monochromatic light with a wavelength of 865 nm (STEP-technology [23]). For the measurement, the samples are filled in rectangular cuvettes which are placed horizontally on a rotating disk. During the centrifugation the transmission of the light is measured over the entire sample height in defined time steps. A part of the light is reflected and absorbed by the particles and the walls of the cuvette. Changes of the local particle concentration over time caused by particles settling in radial direction to the bottom of the cuvette lead to spatially- and time-dependent changes of the

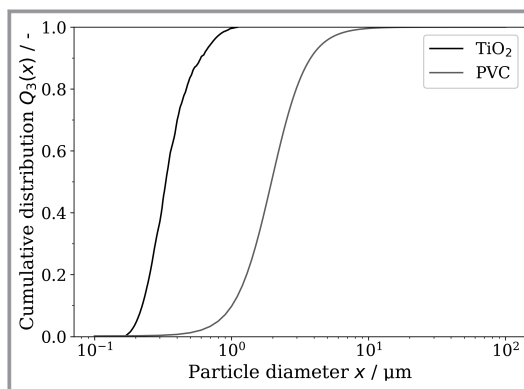


Figure 4. Particle size distribution of TiO₂ and PVC.

transmission. A more detailed description of the measurement principle can be found in [24].

As shown in Fig. 5, the transmission profile has three characteristic sections. The first section (I) represents the gas phase above the sample. Here, the measured transmission equals the transmission of the light after passing through the cuvette. The second section (II) covers the time-dependent sedimentation process. At the start of the measurement, the transmission is reduced at the radial position of the meniscus caused by light reflected and absorbed by particles in the sample. Over time, the particles settle towards the bottom of the cuvette and the clarifying of the fluid leads to an increasing transmission. The progress of change in the transmission profile includes the type of settling phenomena: In the case of hindered settling there is a pronounced phase separation of two zones, one containing the clarified fluid where the transmission is high and one containing the slurry where the transmission is low. The transition of these two zones is abrupt which leads to a nearly vertical line in the transmission profile. During centrifugation the radial position of the phase boundary between clarified liquid and suspension moves in radial direction towards the bottom of the cuvette. In contrast, if swarm sedimentation is present, the transition

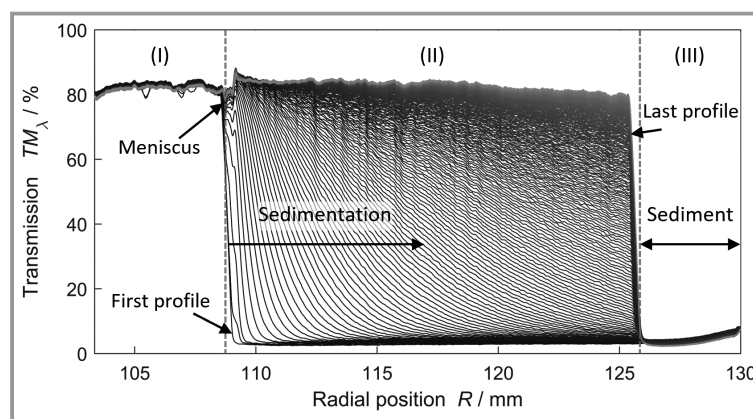


Figure 5. Transmission profile of a measurement with the LUMiSizer[®] with three characteristic sections: (I) the gas phase, (II) the sedimentation process and (III) the sediment zone.

from clarified liquid to slurry is less sharp. The third section (III) represents the sediment zone. Here, the settled particles accumulate and form a sediment. As there is almost no light passing through the sediment which leads to a transmission close to zero.

Using the measured transmission profile, the fitting parameters of the approach by Michaels and Bolger [14] (see Eq. (7)) can be derived using two different methods. The first method makes use of the phase separation when a clear phase boundary between clarified liquid and suspension occurs (vertical transmission profiles). This method measures the radial position of the phase boundary at a determined light intensity in correlation to the measurement time. With the measured data it is possible to calculate velocity of the phase separation. The variation of the solids volume fraction allows to fit the empirical parameters of the hindered settling function to the experimental data according to Eq. (7). For the calculation of the settling velocity according to Stokes, the median particle size $x_{50,3}$ is used which can be determined by laser diffraction analysis or with the LUMiSizer® itself by diluting the slurry as low as possible and assuming Stokes [12].

While it is reasonable to assume hindered settling at high solids volume fractions and thus use the local temporal change of the separation level to calculate the settling velocity, for less concentrated slurries segregation of particles may occur. Here, particles settle according to their size. In this case, it would be necessary to determine a hindered settling function for each particle size class. For this purpose, the description of material behavior requires a particle size dependent hindered settling function which can be derived by the measured settling velocity distribution according to the measurement principle of constant time or constant position [24]. Fig. 6a shows the cumulative distribution of the settling velocity for slurries of different solids volume fraction. With increasing solids volume fraction the particles settle more slowly. Low concentrated slurries show a broad settling velocity distribution that becomes narrower with increasing solids volume fraction. This indicates a shift from particle size dependent settling to hindered settling.

Both methods allow the determination of the hindered settling function (see Fig. 6b). The settling velocity of each solids volume fraction is related to the Stokes' settling velocity according to Eq. (7). With increasing solids volume fraction the settling velocity decreases and correspondingly the hindered settling factor decreases.

3.2 Compression Resistance

To describe the compression behavior with the approach of Green et al. [15], the compression resistance p_s , the empirical parameters p_1 , p_2 and the gel point ϕ_{gel} have to be derived by lab experiments (see Eq. (8)). These experiments are conducted with a beaker centrifuge (HERMLE Labor-technik GmbH). For the experiments, the sample is centrifuged until there are no more changes in the height of the sediment at a constant rotational speed which means that the state of equilibrium for the consolidation of the sediment is reached. In the next step the compressed sediment is cut into slices of a defined height using a sediment cutting setup. Using a cake cutting device the sediment is divided into slices with a defined height h_k whose total mass and solids mass fraction is obtained gravimetrically. According to Reinach [25], the compression resistance p_s of slice k is calculated by the following equation:

$$p_{s,k} = \omega^2 \frac{(\rho_s - \rho_l)}{\rho_l} \frac{4}{A} \left(\sum_{j=1}^{k-1} R_j \Delta m_{s,j} + \frac{R_k \Delta m_{s,k}}{2} \right) \quad (12)$$

Here, A is the cross-section area of the beaker, j is the index of the slice above the considered slice k , R is the radial position and Δm_s the mass of the respective layer. With a non-linear curve fit the empirical parameters of the approach by Green et al. [15] are obtained. Compared to other methods, for example, the compression permeability (CP) cell [26], this approach has the advantage that the formed sediment in the beaker centrifuge is representative for the sediment formed in a decanter centrifuge as the

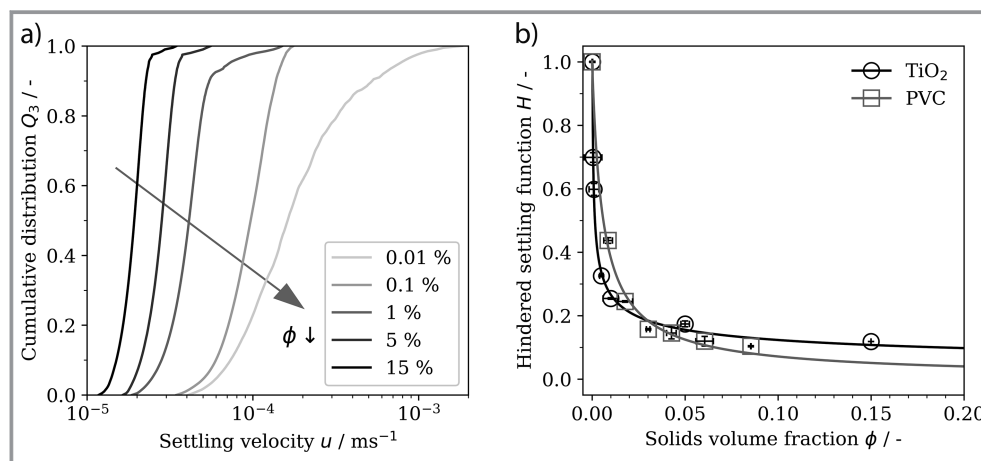


Figure 6. Derivation of the hindered settling function: a) shows the settling velocities of TiO₂ dependent on the solids volume fraction. The higher the solids content, the more the particles hinder each other. As a result, the settling velocity decreases with increasing solids volume fractions. b) Shows the hindered settling functions of TiO₂ and PVC according to Michaels and Bolger [14].

particle orientation, hydrodynamic interactions and segregation during the sedimentation are considered. Fig. 7 shows the compression resistance plotted against the solid volume fraction. Here, TiO_2 and PVC show different compression behaviors. While TiO_2 compresses steadily for a rising compression resistance, PVC compresses mainly at a compression resistance $\rho_s < 20\,000$ Pa. At a higher compression resistance the solids volume fraction barely changes and a nearly steady state is reached at $\phi \approx 0.65$. An explanation for the different compression behavior is the different particle size distribution whereby the median particle size of PVC is $x_{50,3} = 1.96\ \mu\text{m}$ and of TiO_2 is $x_{50,3} = 0.33\ \mu\text{m}$. The gel point of TiO_2 is $\phi_{\text{gel}} = 0.35$ whereas for PVC a gel point of $\phi_{\text{gel}} = 0.45$ is determined.

3.3 Measuring Yield Loci

Ring shear testers allow the characterization of the sediment concerning its flow behavior as well as the investigation of

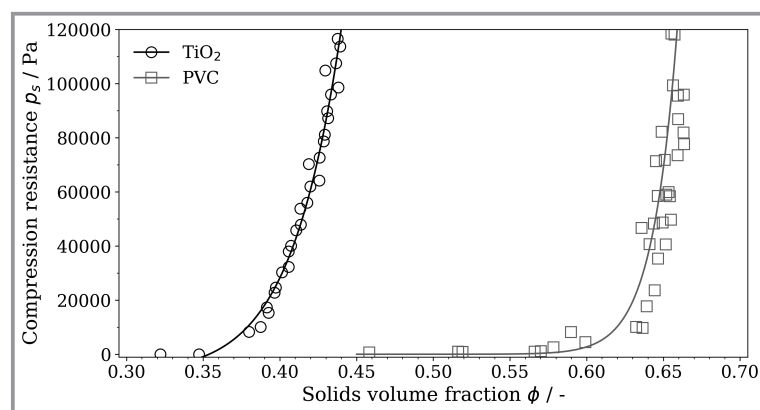


Figure 7. Consolidation functions of TiO_2 and PVC according to Green et al. [15].

the influence of shear on sediment compression. A ring shear tester (RST.01-pc from Dietmar Schulze Schüttgutmesstechnik) and a shear cell modified by Hammerich et al. [16] for liquid-saturated sediment with a saturation of $S = 1$ were used to investigate the materials TiO_2 and PVC. In the shear cell, the particles are held back by the filters and membranes while the liquid can flow out of and back into the bulk material through drainage channels. Both samples were pre-compacted before shearing.

Fig. 8a shows the course of the shear stress and the sediment height of a liquid-saturated TiO_2 sediment during a shear test with an average shear rate of $\bar{v}_{\text{shear}} = 0.001\ \text{m s}^{-1}$. Precompression took place at $\sigma_{\text{pre}} = 80\,400$ Pa. The shear stress profile of the liquid-saturated sediment resembles that from bulk mechanics (Fig 2). In addition, the sediment height is shown. During shearing, the shear stress increases until a steady state is reached where at the same time the sediment height significantly decreases. After that, the system relaxes until the shear stress is reduced to $\tau = 0$ Pa. Then, a rearrangement of the sediment occurs and the sediment height increases. Afterwards, the selected normal stress for the next shear process is set and the sediment is compressed again. This is recognizable by the renewed decrease in sediment height.

The yield point measurements are conducted for three different normal stresses, as shown in Fig. 8b. The shearing takes place at 28 100 Pa, 48 200 Pa, and 68 300 Pa. The course of the stress conditions of TiO_2 and PVC can both be described by a linear function of the normal stress. When extrapolating the shear stress to a normal stress of $\sigma_0 = 0$ Pa the shear stress does not pass the origin but intersect the ordinate at values $\tau > 0$. Thus, the sediments exhibit internal strength and are cohesive.

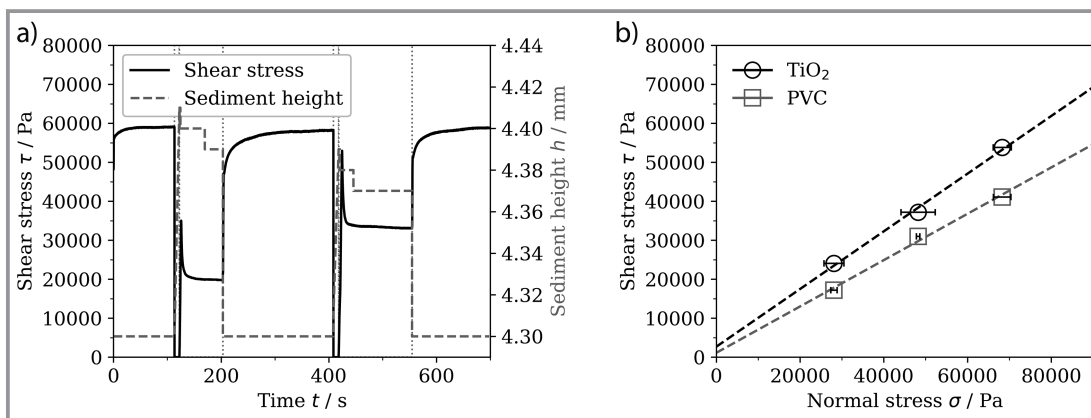


Figure 8. Shear stress: a) shows the shear stress and sediment height as a function of time of a liquid-saturated sediment of TiO_2 and water. There are three characteristic sections: (I) the pre-conditioning, (II) the relaxation and (III) the actual shear experiment. b) Shows the comparison of the shear stress as a function of the normal stress during incipient flow for the materials TiO_2 and PVC.

4 Simulation

To validate the methods of the material characterization, the results of the multi-compartment model are compared to data obtained by experiments on a lab scale decanter centrifuge with the material PVC in form of a PVC-water slurry. The diameter of the bowl is $d_{bo} = 0.08$ m, the solids volume fraction of the feed is $\phi_f = 4.4$ vol % and the pool depth is $h_w = 0.012$ m.

Fig. 9 shows the solids volume fraction of the sediment and the centrate in correlation to the centrifugal number and volumetric flow rate for both the simulation and the experimental data. Regarding the sediment, the solids content increases at higher centrifugal numbers caused by the increasing centrifugal pressure on the sediment which leads to a more compacted sediment. Additionally, more particles are separated due to the increasing settling velocity of the particles. The throughput, on the other hand, has no significant impact on the sediment which shows in both the experimental data and the simulation. In general, the simulation is in good agreement with the experimental data which proves that the presented methods in Sects. 3.2 and 3.3 are adequate to characterize the compaction behavior of a material. The deviation between simulation and experimental data is less than 5 vol % which is within the acceptable margin of error.

Regarding the centrate, the solids content decreases for increasing centrifugal numbers due to the previously mentioned increasing settling velocity of the particles. Furthermore, an increase of the throughput results in less time for the particles to settle and thus a worse separation result. This physical behavior is also considered in the simulation. While the simulation generally shows a good agreement with the experimental data, the simulation tends to slightly overestimate the solids content of the centrate in particular for lower solids content. A possible explanation for this is a shift from hindered settling to swarm settling occurring at

lower solids contents. As described in Sect. 2.1, swarm settling describes hydrodynamic effects which leads to faster settling particles. Currently, solely hindered settling is assumed in the multi-compartment model where all particles settle with a mean settling velocity. Thus, the implementation of a settling velocity distribution instead would improve the accuracy of the model in particular for lower solids content when swarm settling occurs. Despite this, the deviation between simulation and experimental data is below 2 vol % which allows for an adequate prediction of the separation result.

To discuss the scale up capability of the presented methods, a theoretical scale up from lab scale to industrial scale is conducted. Here, the industrial scale machine and operating parameters are chosen based on an apparatus typically used for the separation process. On the industrial scale decanter centrifuge higher centrifugal numbers and throughputs are achievable due to the bigger dimensions. While an experimental validation for the industrial scale centrifuge is not part of this work, Menesklou et al. [10] prove in their work that the simulation result of the scale up achieved by the described methods is in good agreement with the experimental data for calcium carbonate-water slurries.

Fig. 10 compares the separation result of a lab and an industrial scale decanter centrifuge. Referring to the lab scale centrifuge with a throughput of $0.03 \text{ m}^3 \text{ h}^{-1}$ and $0.06 \text{ m}^3 \text{ h}^{-1}$, a similar separation result can be achieved on the industrial scale centrifuge for a throughput of $0.8 \text{ m}^3 \text{ h}^{-1}$ and $1.4 \text{ m}^3 \text{ h}^{-1}$, respectively which is demonstrated in their comparable solids content of the centrate. While the separation result is similar for both scales, there is a shift in the solids content of the sediment. Compared to the lab scale centrifuge ($h_w = 0.012$ m), the industrial scale centrifuge ($h_w = 0.064$ m) has a deeper pool and allows a higher throughput. Consequently, a higher sediment builds up in the industrial scale centrifuge which leads to a higher centrifugal pressure on the sediment and thus to a stronger consolidation.

Overall, the results show that it is possible to simulate solid bowl centrifuges with an adequate accuracy based on a material characterization determined by lab scale experiments. Additionally, the material characterization is scalable which allows for predictions of the separation result of industrial scale solid bowl centrifuges.

5 Outlook

With the presented methods it is possible to characterize materials and derive material functions in lab scale experiments to describe

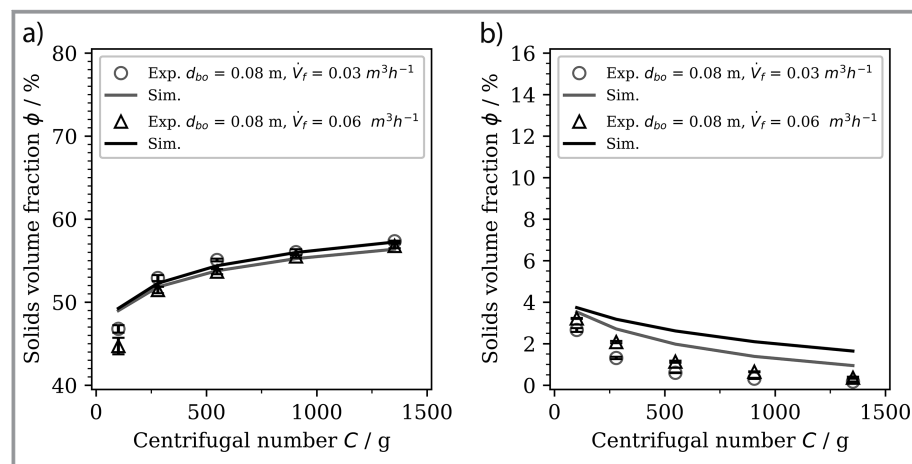


Figure 9. Solids volume fraction of the sediment (a) and centrate (b) for two throughputs and different centrifugal numbers. Here, the experimental data is compared to the results of the simulation for the material PVC.

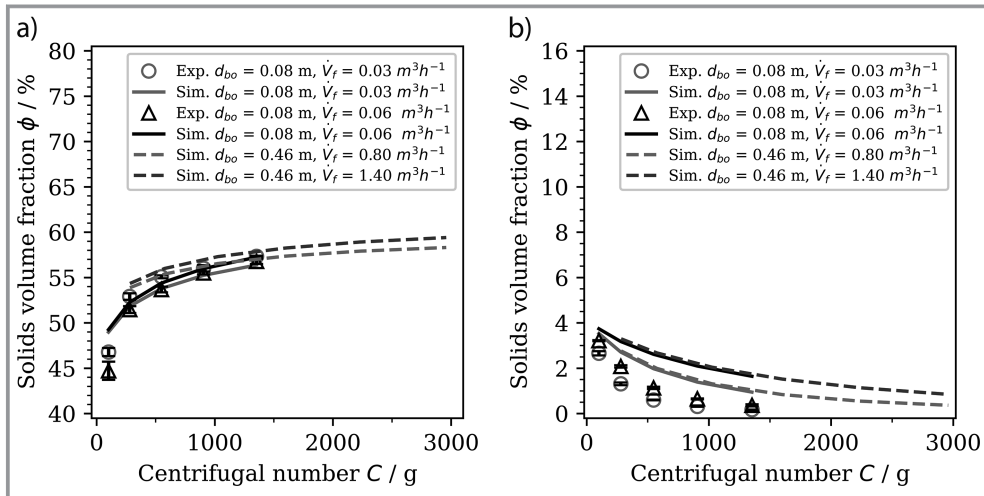


Figure 10. Solids volume fraction of the sediment (a) and centrate (b) for two centrifuges of different scale. Here, the separation result of a lab scale centrifuge ($d_{bo} = 0.08$ m, $h_w = 0.012$ m) and an industrial scale centrifuge ($d_{bo} = 0.46$ m, $h_w = 0.064$ m) for the material PVC.

the material behavior. Implemented in a real-time multi-compartment model, the simulation is in good agreement with the experimental data. While the methods are already being successfully used it is planned to extend them by adding control approaches and optimize them by combining the multi-compartment model with artificial intelligence. Furthermore, the inclusion of the settling velocity distribution could further improve the accuracy of the simulation. In addition, the model presented for the decanter centrifuge can be transferred to other separating devices. These are intended to represent the solid-liquid separation process both as standalone units and within the process chain. This would allow the comparison of different separation apparatuses and the determination of the most suitable separation apparatus for the regarded process based on lab experiments and the derivation of material functions.

The authors thank the BASF SE, the Forschungs-Gesellschaft Verfahrens-Technik e.V. (GVT) and the German Federal Ministry for Economic Affairs and Energy (BMWi) via Forschungszentrum Jülich GmbH (FZJ) for founding their research. The authors also thank their students Robin Jakobi and Mohamad Moslemani for their work in the laboratory. Open access funding enabled and organized by Projekt DEAL.

Symbols used

A	[m ²]	cross-section area
B_c	[m]	screw width
c_D	[-]	drag coefficient
C	[-]	centrifugal number
g	[m s ⁻²]	gravitational acceleration
h	[m]	height

H	[-]	hindered settling function
k	[-]	transport efficiency
Δl	[m]	compartment length
m	[kg]	mass
Δn	[s ⁻¹]	differential speed
p_1, p_2	[Pa], [-]	fit parameter
ρ_s	[Pa]	compression resistance
Q_3	[-]	cumulative distribution
r_1, r_2, r_3	[-]	fit parameter
R	[m]	radius
Re	[-]	Reynolds number
S	[-]	saturation
t	[s]	time
T	[-]	grade efficiency
TM_λ	[%]	transmission
u	[m s ⁻¹]	settling velocity
\dot{V}	[m ³ s ⁻¹]	volumetric flow rate
v_{shear}	[m s ⁻¹]	shear rate
\bar{v}_{tr}	[m s ⁻¹]	solids transport velocity
x_p	[m]	particle diameter

Greek letters

α	[°]	screw pitch angle
η	[Pa s]	dynamic viscosity
ρ	[kg m ⁻³]	density
σ	[Pa]	normal stress
τ	[Pa]	shear stress
ϕ	[-]	solids volume fraction
ω	[s ⁻¹]	angular velocity

Subscripts

0	initial condition
50,3	mass-based median
bo	bowl

f	feed
gel	gel point
i	compartment index
j,k	slice index
l	liquid
p	particle
pre	precompression
s	solid/sediment
Stokes	Stokes condition
w	weir

Abbreviations

CP	compression permeability
PVC	polyvinyl chloride
TiO ₂	titanium dioxide

References

- [1] W. H. Stahl, *Industrie-Zentrifugen*, DrM Press, Landau **2004**.
- [2] C. M. Ambler, *Chem. Eng. Prog.* **1952**, *48*, 150–158.
- [3] C. M. Ambler, *J. Biochem. Microbiol. Technol. Eng.* **1959**, *1* (2), 185–205. DOI: <https://doi.org/10.1002/JBMTE.390010206>
- [4] R. Wakeman, S. Tarleton, *Solid/Liquid Separation: Scale-Up of Industrial Equipment*, Elsevier, Amsterdam **2005**.
- [5] W. Leung, *Industrial Centrifugation Technology*, McGraw-Hill, New York **1998**.
- [6] W. Leung, *Sep. Purif. Technol.* **2016**, *171*, 69–79. DOI: <https://doi.org/10.1016/j.seppur.2016.07.010>
- [7] H. K. Baust, S. Hammerich, H. König, H. Nirschl, M. Gleiß, *Separations* **2022**, *9* (9), 248. DOI: <https://doi.org/10.3390/separations9090248>
- [8] M. Gleiss, S. Hammerich, M. Kespe, H. Nirschl, *Chem. Eng. Technol.* **2018**, *41* (1), 19–26. DOI: <https://doi.org/10.1002/ceat.201700113>
- [9] M. Gleiß, *Dynamische Simulation der mechanischen Flüssigkeitsabtrennung in Vollmantelzentrifugen*, Ph.D. Thesis, Karlsruher Institut für Technologie **2018**.
- [10] P. Menesklou, T. Sinn, H. Nirschl, M. Gleiss, *Minerals* **2021**, *11* (2), 229. DOI: <https://doi.org/10.3390/min11020229>
- [11] M. Stieß, *Mechanische Verfahrenstechnik 2*, Springer, Berlin **1994**.
- [12] G. G. Stokes, *Mathematical and Physical Papers*, Vol. 3, Cambridge University Press, Cambridge **2009**.
- [13] J. F. Richardson, W. N. Zaki, *Chem. Eng. Sci.* **1954**, *3* (2), 65–73. DOI: [https://doi.org/10.1016/0009-2509\(54\)85015-9](https://doi.org/10.1016/0009-2509(54)85015-9)
- [14] A. Michaels, J. Bolger, *Ind. Eng. Chem. Fundam.* **1962**, *1* (1), 24–33. DOI: <https://doi.org/10.1021/i160001a004>
- [15] M. D. Green, M. Eberl, K. A. Landmann, *AIChE J.* **1996**, *42* (8), 2308–2318. DOI: <https://doi.org/10.1002/aic.690420820>
- [16] S. Hammerich, A. D. Stickland, B. Radel, M. Gleiss, H. Nirschl, *Particuology* **2019**, *51*, 1–9. DOI: <https://doi.org/10.1016/j.partic.2019.10.005>
- [17] A. Erk, *Rheologische Eigenschaften feindisperser Suspensionen in Filter und Zentrifugen*, Ph.D. Thesis, Karlsruher Institut für Technologie **2006**.
- [18] K. Raschka, H. Buggisch, *Aufbereit.-Tech.* **1992**, *33* (3), 132–139.
- [19] T. Mladenchev, *Modellierung des Filtrations- und Fließverhaltens von ultrafeinen, kompressiblen, flüssigkeitsgesättigten Partikelpackungen*, Ph.D. Thesis, Otto-von-Guericke-Universität Magdeburg **2007**.
- [20] D. Schulze, *Powders and Bulk Solids*, Springer, Berlin **2008**.
- [21] J. Vaxelaire, J. Olivier, *Drying Technol.* **2014**, *32* (1), 23–29. DOI: <https://doi.org/10.1080/07373937.2013.807282>
- [22] A. Erk, B. Luda, *Chem. Ing. Tech.* **2003**, *75* (9), 1250–1254. DOI: <https://doi.org/10.1002/cite.200303260>
- [23] T. Detloff, T. Sobisch, D. Lерche, *Powder Technol.* **2007**, *174*, 50–55. DOI: <https://doi.org/10.1016/j.powtec.2006.10.021>
- [24] D. Lерche, *J. Dispersion Sci. Technol.* **2002**, *23* (5), 699–709. DOI: <https://doi.org/10.1081/DIS-120015373>
- [25] H. Reinach, *Gleichgewicht and Kinetik der Preßentfeuchtung im Zentrifugalfeld einer Becherzentrifuge und in einer Stempelpresse dargestellt an einem stark kompressiblen Kaolinschlamm*, Ph.D. Thesis, Universität Karlsruhe **1992**.
- [26] C. M. Alles, *Prozeßstrategien für die Filtration mit kompressiblen Kuchen*, Ph.D. Thesis, Universität Karlsruhe **2000**.

DOI: 10.1002/cite.202200117

Model-based Scale Up of Solid Bowl Centrifuges Using Experimentally Determined Material Functions

Ouwen Zhai*, Helene Baust, Marco Gleiß, Hermann Nirschl

Research Article: The scale up of solid bowl centrifuges is a major challenge due to the complex process and material behavior. Common approaches for the scale up are time-consuming and costly. An alternative approach is to derive the material behavior by laboratory experiments and use a numerical model to achieve an improved scale up of solid bowl centrifuges.

